ACS Sustainable Chemistry & Engineering

Research Article

pubs.acs.org/journal/ascecg

Compression-Induced Open Circuit Voltage Increase in All-Polymer Solar Cells with Lithium Fluoride Nanolayers

Sooyong Lee,[†] Sungho Nam,[†] Hwajeong Kim,[†,‡] and Youngkyoo Kim*,[†]

[†]Organic Nanoelectronics Laboratory, Department of Chemical Engineering, Kyungpook National University, Daegu 702-701, Republic of Korea

[‡]Research Institute of Advanced Energy Technology, Kyungpook National University, Daegu 702-701, Republic of Korea

ABSTRACT: We report an open circuit voltage (V_{OC}) increase by physical pressing of all-polymer solar cells with bulk heterojunction (BHJ) films of poly(3-hexylthiophene) and poly(9,9-dioctylfluorene-co-benzothiadiazole). When compression force was applied in the direction normal to the BHJ film plane, V_{OC} was increased for all-polymer solar cells with a lithium fluoride (LiF) nanolayer (~1 nm thick) between the BHJ and cathode layers. However, V_{OC} was rather decreased for all-polymer solar cells without the LiF layer upon compression. Interestingly, the V_{OC} change (both increase and decrease) was linearly proportional to the intensity of pressing (compression) forces. The reason for the V_{OC} increase in the device with the LiF layer has been assigned to the improved LiF dipole alignment and interfacial contacts during rearrangement of the nanolayer (LiF) nanomorphology upon pressing.

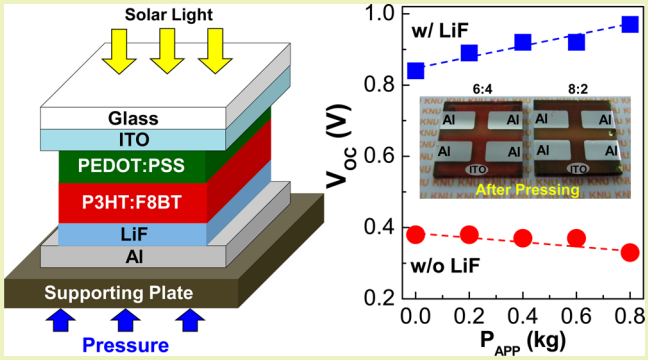

KEYWORDS: *All-polymer solar cells, Open circuit voltage, Pressing, Dipole, Interfacial contact*

INTRODUCTION

Since the early breakthroughs in bulk heterojunction (BHJ) organic solar cells,[1−8] their power conversion efficiency (PCE) has recently reached 8−10% by employing new organic materials and/or inverted/tandem device structures.[9−16] Most of these high PCE organic solar cells are fabricated with the BHJ films of electron-donating (p-type) polymers and electron-accepting (n-type) fullerene derivatives, which can be prepared by wet-coating processes such as spin-coating, spray-coating, inkjet-coating, slot-die coating, etc at room temperature.[17,18]

However, the stability (lifetime) issue is still unsettled for the polymer:fullerene solar cells, and the morphological instability in the polymer:fullerene mixtures has been suggested as one of major reasons for their low stability.[19−23] On this account, all-polymer solar cells have been increasingly highlighted because they have an all-polymer BHJ layer that replaces the crystallizable small molecule (fullerene derivative) with an electron-accepting polymer.[2,24−31] Disappointedly, however, the PCE of all-polymer solar cells is yet far lower than that of polymer:fullerene solar cells, which can be mainly ascribed to the too well-mixing between the electron-donating polymer chains and the electron-accepting polymers leading to poor charge percolation paths.[24−26]

Hence, in order to maximize the charge transport and collection in all-polymer solar cells, a lithium fluoride (LiF) layer has been inserted between the BHJ layer and the electron-collecting electrode because built-in electric fields (a driving force for charge collection in short circuit condition) in all-polymer solar cells can be increased by the LiF layer insertion due to the dipole-induced energy band alignment (shift).[26,32−34] In these previous works, the LiF layer was simply deposited by thermal evaporation and followed by deposition of electron-collecting electrodes, but no attempt has been tried to improve the interfaces between the LiF layer and the BHJ layer or the electron-collecting electrode.

In this work, we attempted to make better LiF interfaces by physically pressing both sides of the top and bottom electrodes (i.e., compression of devices) in normal-type all-polymer solar cells with the BHJ films of p-type poly(3-hexylthiophene) (P3HT) and n-type poly(9,9-dioctylfluorene-co-benzothiadiazole) (F8BT) (Figure 1a). For better understanding of the pressing effect, the pressing force (pressure) was gradually changed during measurement under an air mass 1.5G condition (100 mW/cm^2). Results showed that open circuit voltage (V_{OC}) was impressively increased by pressing all-polymer solar cells with the LiF layer, and the V_{OC} increment was proportional to the intensity of pressing (compression) forces. However, interestingly, all-polymer solar cells without the LiF layer showed rather decreased V_{OC} trends.

EXPERIMENTAL SECTION

Materials and Solutions. The P3HT polymer (weight-average molecular weight = 50 kDa; polydispersity index = 2.2) was used as received from Rieke Metals (Nebraska, U.S.A.), while the F8BT

Received: May 9, 2013
Revised: July 26, 2013
Published: August 8, 2013

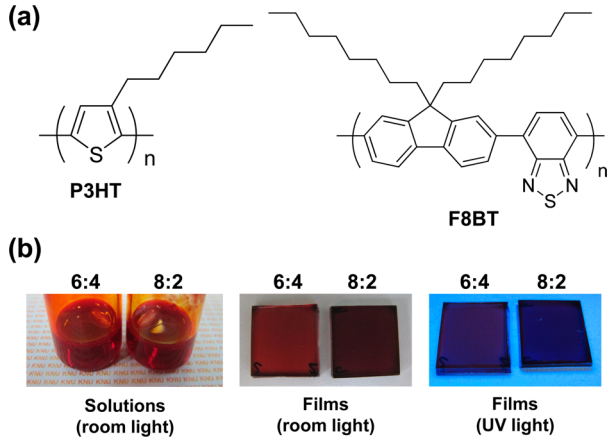

Figure 1. (a) Chemical structure of P3HT and F8BT. (b) Photographs of blend solutions (left), blend films under room right (middle), and blend films under UV light (365 nm) (right). The weight ratio of P3HT and F8BT is given on top of each photograph.

polymer (weight-average molecular weight = 46 kDa) was supplied from American Dye Sources (Quebec, Canada). Two binary blend solutions of P3HT and F8BT (P3HT:F8BT = 8:2 and 6:4 by weight) were prepared using chlorobenzene as a solvent at a solid concentration of 40 mg/mL.

Thin Film and Device Fabrication. To fabricate all-polymer solar cells, indium–tin oxide (ITO)-coated glass substrates were patterned to have 8 mm × 12 mm ITO strips by employing a photoengraving technology (photolithography and etching processes). The patterned ITO–glass substrates were cleaned with isopropyl alcohol and acetone, followed by UV–ozone treatment. On top of the cleaned ITO–glass substrates, a hole-collecting buffer layer (HCBL) was spin-coated using poly(3,4-ethylenedioxythiophene):poly(styrenesulfonate) (PEDOT:PSS) (PH500, HC Starck) solution and then thermally annealed at 230 °C for 15 min. Next, the P3HT:F8BT blend films (thickness = 90 nm) were spin-coated on the PEDOT:PSS layer (thickness = 40 nm) that was coated on the ITO–glass substrates, followed by soft-baking at 50 °C for 15 min. These samples were loaded into a vacuum chamber equipped inside an argon-filled glovebox for top electrode deposition. A LiF nanolayer (~1 nm) was first deposited on one set of the active layer (P3HT:F8BT)-coated samples by thermal evaporation, followed by deposition of aluminum (Al) electrodes. Only Al electrodes (without LiF) were deposited on another set of the samples. Then all devices were thermally annealed at 150 °C for 10 min. The active area of all devices was 0.09 cm^2.

Measurements. To measure current density–voltage (J-V) curves of all-polymer solar cells, we setup a specialized sample holder system of which pressing pistons were sealed, and its inner environment became inert by purging argon gas. After loading the devices into the sample holder inside an argon-filled glovebox, the sample holder was taken out of the glovebox and mounted on a home-built measurement stage under a solar simulator (92250A-1000, Newport Corp.). Next, the light J-V curves under 1 sun condition (air mass 1.5G, 100 mW/cm^2) were measured using an electrometer (Keithley 2400) for all-polymer solar cells that were pressed by varying the pressing force up to 0.8 kg (pressure = 8.9 kg/cm^2) (Figure 1b).

RESULTS AND DISCUSSION

As shown in Figure 1b, both P3HT and F8BT polymers were well dissolved in chlorobenzene, and no phase separation was observed in solutions for the two compositions. After spin-coating, we could obtain well-coated uniform films without any microscale phase segregation (see the middle photographs in Figure 1b). However, the color of films was different depending on the polymer composition: The higher the P3HT content, the darker the film color. In particular, almost no photoluminescence could be observed from the P3HT:F8BT blend films under illumination of UV lamp (wavelength = 365 nm), which supports efficient charge separation between donor (P3HT) and acceptor (F8BT) phases on a nanoscale in the present P3HT:F8BT films as observed in our previous reports.[26,30,31] Using these blend films, we fabricated all-polymer solar cells with or without the LiF layer in order to

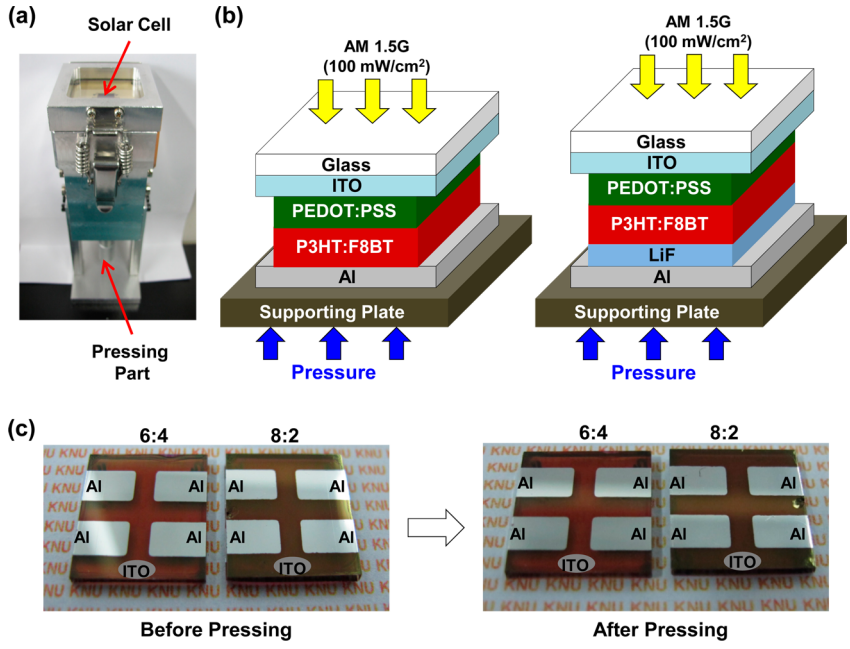

Figure 2. (a) Photograph of sample holder that has a pressing component on its bottom part and Ar environment in its inner part where solar cells are mounted. (b) Illustration for compressing experiment of all-polymer solar cells under air mass (AM) 1.5G condition (1 sun, 100 mW/cm^2). (Left) All-polymer (P3HT:F8BT) solar cell without the LiF layer. (Right) All-polymer solar cell with the LiF layer. (c) Photographs for the devices with the LiF layer before and after pressing. The weight ratio of P3HT and F8BT is given on top of each photograph.

examine the influence of the LiF layer that has a strong dipole moment (D = 6.284).[41] These all-polymer solar cells were loaded into a sample holder equipped with a pressing part on the bottom part of which the inner part is charged with argon gas (Figure 2a). Then we measured current density−voltage (J-V) curves by varying pressing forces under illumination of simulated solar light (100 mW/cm^2) (Figure 2b). Here, we note that the devices were almost not hurt by pressing as observed from photographs in Figure 2c.

As shown in Figure 3a, the light J-V curve of the device (P3HT:F8BT = 6:4) without the LiF layer became worse as the

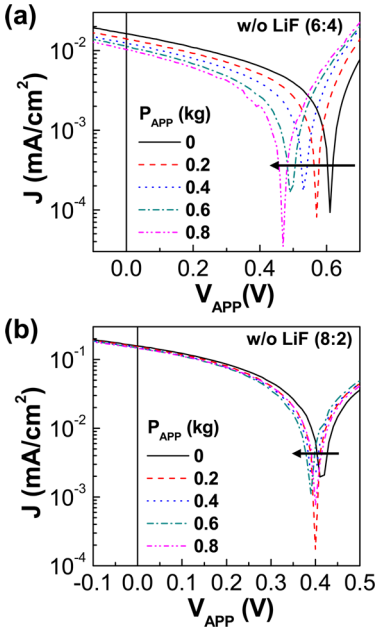

Figure 3. Light J-V curves according to the pressing force (P_{APP}): (a) 6:4 (P3HT:F8BT) device without the LiF layer and (b) 8:2 device without the LiF layer. Arrows denote the direction of increasing P_{APP}.

applied pressing force (P_{APP}) increased. A pronounced open circuit voltage (V_{OC}) reduction (from 0.61 V at P_{APP} = 0 kg to 0.47 V at P_{APP} = 0.8 kg) was measured in the presence of the similar short circuit current density (J_{SC}) decrease. In the case of the 8:2 devices (Figure 3b), the device pressing resulted in the similar deterioration in device performances, even though the extent of deterioration was relatively smaller for the 8:2 devices than the 6:4 devices. Here, we note that the J_{SC} value without pressing (P_{APP} = 0 kg) was higher for the 8:2 device than the 6:4 device, but the V_{OC} trend was reversed (Table I). However, the fill factor (FF) was not greatly changed (<4% for the 6:4 devices and <8% for the 8:2 devices), which may reflect no intrinsic change in the BHJ morphology in the P3HT:F8BT layers. In contrast to the FF trend, the series resistance (R_S) was noticeably increased by ∼83% for the 6:4 devices and ∼29% for the 8:2 devices between P_{APP} = 0 kg and P_{APP} = 0.8 kg). As a result, the power conversion efficiency (PCE) was decreased by ∼66% for the 6:4 devices and ∼50% for the 8:2 devices. Hence, we think that the interface between the active layer (P3HT:F8BT) and the Al electrode might be degraded by pressing.

Interestingly, however, we found that the V_{OC} value of the 6:4 devices with the LiF layer was apparently increased by increasing the pressing force (from 0.78 V at P_{APP} = 0 kg to 0.96 V at P_{APP} = 0.8 kg), though the V_{OC} increment was not

Table I. Summary of Solar Cell Parameters According to Pressing Forces (P_{APP}) for All-Polymer (P3HT:F8BT) Solar Cells with (w/) or without (w/o) the LiF Nanolayer

		P3HT:F8BT (6:4)		P3HT:F8BT (8:2)	
parameters	P_{APP} (kg)	w/ LiF	w/o LiF	w/ LiF	w/o LiF
J_{SC}(mA/cm^2)	0	0.487	0.016	0.345	0.153
	0.2	0.471	0.014	0.340	0.145
	0.4	0.469	0.012	0.337	0.144
	0.6	0.485	0.011	0.329	0.118
	0.8	0.477	0.010	0.324	0.115
V_{OC} (V)	0	0.78	0.61	0.85	0.38
	0.2	0.82	0.57	0.89	0.38
	0.4	0.83	0.53	0.92	0.37
	0.6	0.95	0.49	0.92	0.37
	0.8	0.96	0.47	0.97	0.33
FF (%)	0	25.2	26.5	27.5	26.6
	0.2	24.9	27.1	27.8	26.3
	0.4	25.1	27.4	28.1	26.5
	0.6	25.0	26.6	27.9	28.1
	0.8	24.9	26.4	27.8	28.8
PCE (%)	0	0.096	0.003	0.081	0.015
	0.2	0.096	0.002	0.084	0.015
	0.4	0.098	0.002	0.087	0.014
	0.6	0.115	0.001	0.084	0.012
	0.8	0.114	0.001	0.087	0.011
R_S (kΩ cm^2)	0	15.13	215.62	20.09	22.77
	0.2	19.95	196.22	22.18	27.74
	0.4	19.82	234.95	19.89	26.81
	0.6	22.54	328.30	20.63	26.98
	0.8	21.70	394.99	23.64	29.32

exactly the same as for the pressing force increment (Figure 4a). In particular, the J_{SC} change seemed to be almost marginal (∼2% between P_{APP} = 0 kg and P_{APP} = 0.8 kg) (Table I). This V_{OC} increasing trend upon device pressing was also observed

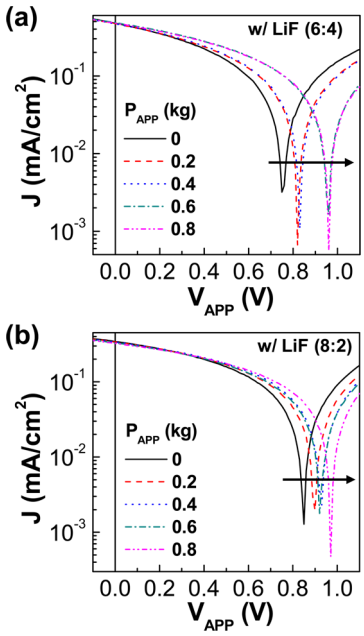

Figure 4. Light J-V curves according to pressing forces (P_{APP}): (a) 6:4 (P3HT:F8BT) device with the LiF layer and (b) 8:2 device with the LiF layer. Arrows denote the direction of increasing P_{APP}.

for the 8:2 devices (from 0.85 V at P_{APP} = 0 kg to 0.97 V at P_{APP} = 0.8 kg) (Figure 4b), in which the J_{SC} value was slightly decreased at P_{APP} = 0.2−0.6 kg but became the same at P_{APP} = 0.8 kg as for the unpressed device (Table I). In addition, the FF values were almost unchanged for the devices with the LiF layer irrespective of the blend composition. As a result, the PCE value was increased by ∼14% for the 6:4 devices and ∼13% for the 8:2 devices (Table I). However, we need to pay attention to the R_S change for the devices with the LiF layer. The R_S value was increased by ∼49% (at P_{APP} = 0.6 kg) for the 6:4 devices, while the R_S increment was ∼18% (at P_{APP} = 0.8 kg) for the 8:2 devices. If we consider only the R_S increase factor, the device performance should be worse in every case when the pressing forces were exerted to the devices. However, the PCE of the device with the LiF layer could be increased due to the V_{OC} increase by pressing the devices. In principle, it is reasonable to accept the improved device performance because the built-in electric field enhanced by the increased V_{OC} can speed up the charge transport so that the number of charge carriers (electrons and holes) photogenerated by light absorption could be relatively higher for the pressed devices than the unpressed devices.

For the detailed analysis on the V_{OC} increase by pressing, the V_{OC} values were plotted as a function of pressing force. As shown in Figure 5a, the V_{OC} change in the 6:4 devices was

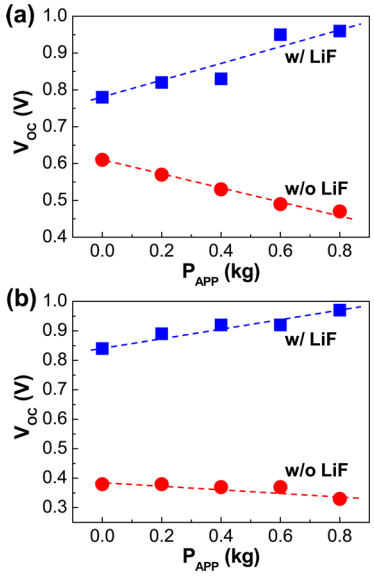

Figure 5. Open circuit voltage (V_{OC}) as a function of pressing force (P_{APP}): (a) 6:4 (P3HT:F8BT) device and (b) 8:2 (P3HT:F8BT) device. The "w/" and "w/o" stand for "with" and "without", respectively. The dashed lines represent the linearly fitted results: V_{OC}/P_{APP} = 0.25 (6:4 device with the LiF layer), −0.18 (6:4 device without the LiF layer), 0.15 (8:2 device with the LiF layer), and −0.05 (8:2 device without the LiF layer).

clearly divided into two different trends. The V_{OC} value was linearly *increased* for the device with the LiF layer, whereas it was linearly *decreased* for the device without the LiF layer. Here, it is worthy to note that the V_{OC} change is linear with the pressing force for both increasing and decreasing cases. This trend was similar for the 8:2 devices as shown in Figure 5b. Hence, we can draw a short conclusion that the interfacial change in the devices, whether the LiF layer exists or not, is linearly proportional to the pressing force. The V_{OC} increase per pressing force was V_{OC}/P_{APP} = +0.25 for the 6:4 device with the LiF layer, while it was V_{OC}/P_{APP} = +0.15 for the 8:2 device with the LiF layer. Thus, the V_{OC} of all-polymer solar cells with the LiF layer can be increased by at least 0.15 V by pressing them with P_{APP} = 1 kg. In the case of the devices without the LiF layer, however, the V_{OC}/P_{APP} was −0.18 (6:4 device) and −0.05 (8:2 device), which indicates that pressing all-polymer solar cells without the LiF layer (i.e., only Al electrodes) results in the V_{OC} decrease leading to worsening device performances.

Finally, we tried to get an insight on the reason for the V_{OC} increase by the existence of the LiF layer between the active layer and the Al electrode. As shown in Figure 6a, the

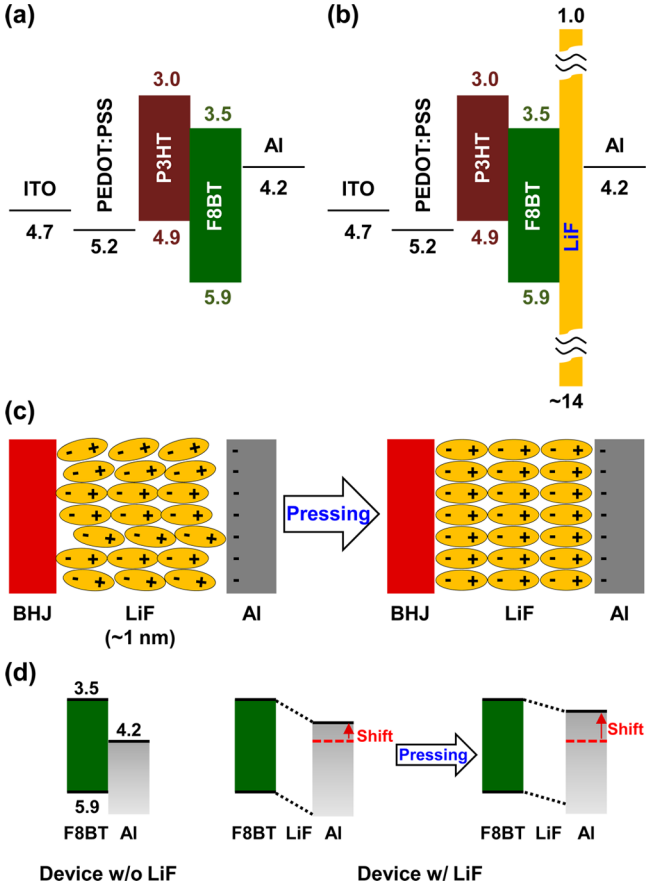

Figure 6. Flat energy band diagram for the device without the LiF layer (a) and with the LiF layer (b). Both energy unit (eV) and minus sign (−) in the numbers were omitted to avoid crowding figures. (c) Illustration for the rearrangement of LiF molecules (dipoles) in the LiF nanolayer between the P3HT:F8BT BHJ layer and the Al electrode by pressing all-polymer solar cells: (left) before pressing and (right) after pressing. (d) Scheme for the work function shift in the Al electrode by the dipole rearrangement upon pressing all-polymer solar cell with the LiF nanolayer.

theoretically calculated V_{OC} value is 1.4 V for the P3HT:F8BT device without the LiF layer.[26,35,36] However, the measured V_{OC} value (maximum here is 0.61 V for the unpressed 6:4 device) was far lower than 1.4 V (Table I), which indicates the presence of huge charge blocking resistance that could not be overcome by the actual built-in voltage (only 1 V if considering the work functions of the PEDOT:PSS layer and the Al electrode). Upon pressing the device with only Al electrodes (without the LiF layer), we can expect that only improvement might be an enhanced physical adhesion between the polymeric

dx.doi.org/10.1021/sc400141q | ACS Sustainable Chem. Eng. 2013, 1, 1280−1285

layer (P3HT:F8BT film) and the metallic layer (Al electrode) if any. However, this adhesion improvement cannot contribute to any V_{OC} increase, although it could lead to the J_{SC} increase under an ideal pressing condition (however, we note that the J_{SC} increase was unable to achieve in the present experiment as summarized in Table I). On the contrary, in the case of the device with the LiF layer, the LiF layer (~1 nm) was formed first on the polymeric BHJ layer (P3HT:F8BT) and then the Al electrode was deposited on top of the preformed LiF layer.[37,38] Hence, we can guess that the thin LiF nanolayer might be thermodynamically imperfect in terms of dipole alignment and interfacial morphology when it comes to the typical surface roughness of the P3HT:F8BT layers.[26,30,31] In addition, the device annealing at 150 °C might cause further unsettlement of the LiF alignment.[26,39] Therefore, as shown in Figure 6c,d, the molecular (dipole) alignment and interfacial contact of the LiF layer could be improved in due course of rearrangement of interface morphology upon pressing. In other words, the pressing force acts as a driving force to heal the interfacial defects around the LiF layer. Here, we note that three LiF molecules might be included in the ~1 nm thick LiF layer because the lattice constant of LiF is ~0.4 nm, though the LiF crystal formation could be imperfect in the thermally deposited LiF layer.[40] As a consequence, the better alignment of LiF dipoles by device pressing is considered to contribute to the recovery of the built-in electric field (more vacuum level alignment) toward a theoretical value (Figure 6d).

CONCLUSIONS

We tried to press all-polymer solar cells by varying pressing forces and found that the V_{OC} value was increased for the device with the LiF layer, but it was decreased for the device without the LiF layer. In particular, the V_{OC} change (both increase and decrease) was linearly proportional to the pressing forces. We found that the V_{OC} enhancement could be possible by 0.15−0.25 V per 1 kg pressing force for all-polymer solar cells with the LiF layer. We concluded that the V_{OC} increase for the devices with the LiF layer is related to the improved LiF dipole alignment and interfacial contacts during the interfacial morphology rearrangement upon pressing (compression). Finally, we expect that the present physical pressing method can be effectively applied for other types of organic solar cells such as polymer:fullerene solar cells, small molecule-based organic solar cells, organic/inorganic hybrid solar cells, etc.

AUTHOR INFORMATION

Corresponding Author

*Email: ykimm@knu.ac.kr. Tel.: +82-53-950-5616.

Notes

The authors declare no competing financial interest.

ACKNOWLEDGMENTS

This work was financially supported by Korean Government grants (Basic Science Research Program 2009-0093819, Basic Research Laboratory Program 2011-0020264, Pioneer Research Center Program 2012-0001262, NRF 2012R1A1B3000523, NRF 2013M4A1039332, and NRF 2012K1A3A1A09027883).

REFERENCES

(1) Sariciftci, N. S.; Smilowitz, L.; Heeger, A. J.; Wudl, F. Photoinduced electron transfer from a conducting polymer to buckminsterfullerene. *Science* **1991**, *27*, 1474−1476.

(2) Granström, M.; Petritsch, K.; Arias, A. C.; Lux, A.; Andersson, M. R.; Friend, R. H. Laminated fabrication of polymeric photovoltaic diodes. *Nature* **1998**, *395*, 257−260.

(3) Shaheen, S. E.; Brabec, C. J.; Sariciftci, N. S. 2.5% efficient organic plastic solar cells. *Appl. Phys. Lett.* **2001**, *78*, 841−843.

(4) Nguyen, L. H.; Hoppe, H.; Erb, T.; Günes, S.; Gobsch, G.; Sariciftci, N. S. Effects of annealing on the nanomorphology and performance of poly(alkylthiophene):fullerene bulk-heterojunction solar cells. *Adv. Funct. Mater.* **2007**, *17*, 1071−1078.

(5) Kim, Y.; Choulis, S. A.; Nelson, J.; Bradley, D. D. C.; Cook, S.; Durrant, J. R. Device annealing effect in organic solar cells with blends of regioregular poly(3-hexylthiophene) and soluble fullerene. *Appl. Phys. Lett.* **2005**, *86*, 063502.

(6) Reyes-Reyes, M.; Kim, K.; Carroll, D. L. High-efficiency photovoltaic devices based on annealed poly(3-hexylthiophene) and 1-(3-methoxycarbonyl)-propyl-1-phenyl-(6,6)C_{61} blends. *Appl. Phys. Lett.* **2005**, *87*, 083056.

(7) Li, G.; Shrotriya, V.; Huang, J.; Yao, Y.; Moriarty, T.; Emery, K.; Yang, Y. High-efficiency solution processable polymer photovoltaic cells by self-organization of polymer blends. *Nat. Mater.* **2005**, *4*, 864−868.

(8) Kim, Y.; Cook, S.; Tuladhar, S. M.; Choulis, S. A.; Nelson, J.; Durrant, J .R.; Bradley, D. D. C.; Giles, M.; McCulloch, I.; Ha, C. S.; Ree, M. A strong regioregularity effect in self-organizing conjugated polymer films and high-efficiency polythiophene:fullerene solar cells. *Nat. Mater.* **2006**, *5*, 197−203.

(9) Peet, J.; Kim, J.; Coates, N. E.; Ma, W. L.; Moses, D.; Heeger, A. J.; Bazan, G. C. Efficiency enhancement in low-band gap polymer solar cells by processing with alkane dithiols. *Nat. Mater.* **2007**, *6*, 497−500.

(10) Kim, J.; Lee, K.; Coates, N. E.; Moses, D.; Nguyen, T.; Dante, M.; Heeger, A. J. Efficient tandem polymer solar cells fabricated by all-solution processing. *Science* **2007**, *317*, 222−225.

(11) Chen, H.; Hou, J.; Zhang, S.; Liang, Y.; Yang, G.; Yang, Y.; Yu, L.; Wu, Y.; Li, G. Polymer solar cells with enhanced open-circuit voltage and efficiency. *Nat. Photon.* **2009**, *3*, 649−653.

(12) Park, S.; Roy, A.; Beaupré, S.; Cho, S.; Coates, N.; Moon, J.; Moses, D.; Leclerc, M.; Lee, K.; Heeger, A. J. Bulk heterojunction solar cells with internal quantum efficiency approaching 100%. *Nat. Photon.* **2009**, *3*, 297−302.

(13) Dou, L.; Gao, J.; Richard, E.; You, J.; Chen, C.; Cha, K. C.; He, Y.; Li, G.; Yang, Y. Systematic investigation of benzodithiophene- and diketopyrrolopyrrole-based low-bandgap polymers designed for single junction and tandem polymer solar cells. *J. Am. Chem. Soc.* **2012**, *134*, 10071−10079.

(14) Dou, L.; You, J.; Yang, J.; Chen, C.; He, Y.; Murase, S.; Moriarty, T.; Emery, K.; Li, G.; Yang, Y. Tandem polymer solar cells featuring a spectrally matched low-bandgap polymer. *Nat. Photon.* **2012**, *6*, 180−185.

(15) He, Z.; Zhong, C.; Huang, X.; Wong, W.; Wu, H.; Chen, L.; Su, S.; Cao, Y. Simultaneous enhancement of open-circuit voltage, short-circuit current density, and fill factor in polymer solar cells. *Adv. Mater.* **2011**, *23*, 4636−4643.

(16) He, Z.; Zhong, C.; Su, S.; Xu, M.; Wu, H.; Cao, Y. Enhanced power-conversion efficiency in polymer solar cells using an inverted device structure. *Nat. Photon.* **2012**, *6*, 591−595.

(17) Søndergaard, R.; Hösel, M.; Angmo, D.; Larsen-Olsen, T. T.; Krebs, F. C. Roll-to-roll fabrication of polymer solar cells. *Mater. Today* **2012**, *15*, 36−49.

(18) Hoth, C. N.; Schilinsky, P.; Choulis, S. A.; Brabec, C. J. Printing highly efficient organic solar cells. *Nano Lett.* **2008**, *8*, 2806−2813.

(19) Jørgensen, M.; Norrman, K.; Gevorgyan, S. A.; Tromholt, T.; Andreasen, B.; Krebs, F. C. Stability of polymer solar cells. *Adv. Mater.* **2012**, *24*, 580−612.

(20) Kim, H.; Shin, M.; Park, J.; Kim, Y. Initial performance changes of polymer/fullerene solar cells by short-time exposure to simulated solar light. *ChemSusChem* **2010**, *3*, 476−480.

(21) Shin, M.; Kim, H.; Park, J.; Nam, S.; Heo, K.; Ree, M.; Ha, C. S.; Kim, Y. Abrupt morphology change upon thermal annealing in poly(3-

hexylthiophene)/soluble fullerene blend films for polymer solar cells. *Adv. Funct. Mater.* **2010**, *20*, 748−754.
(22) Kim, Y.; Nelson, J.; Zhang, T.; Cook, S.; Durrant, J. R.; Kim, H.; Park, J.; Shin, M.; Nam, S.; Heeney, M.; McCulloch, I.; Ha, C. S.; Bradley, D. D. C. Distorted asymmetric cubic nanostructure of soluble fullerene crystals in efficient polymer:fullerene solar cells. *ACS Nano* **2009**, *3*, 2557−2562.
(23) Kim, J.; Lee, S.; Nam, S.; Lee, H.; Kim, H.; Kim, Y. A pronounced dispersion effect of crystalline silicon nanoparticles on the performance and stability of polymer:fullerene solar cells. *ACS Appl. Mater. Interfaces* **2012**, *4*, 5300−5308.
(24) Snaith, H. J.; Arias, A. C.; Morteani, A. C.; Silva, C.; Friend, R. H. Charge generation kinetics and transport mechanisms in blended polyfluorene photovoltaic devices. *Nano Lett.* **2002**, *2*, 1353−1357.
(25) Arias, A. C.; MacKenzie, J. D.; Stevenson, R.; Halls, J. J. M.; Inbasekaran, M.; Woo, E. P.; Richards, D.; Friend, R. H. Photovoltaic performance and morphology of polyfluorene blends: a combined microscopic and photovoltaic investigation. *Macromolecules* **2001**, *34*, 6005−6013.
(26) Kim, Y.; Cook, S.; Choulis, S. A.; Nelson, J.; Durrant, J. R.; Bradley, D. D. C. Organic photovoltaic devices based on blends of regioregular poly(3-hexylthiophene) and poly(9,9-dioctylfluorene-co-benzothiadiazole). *Chem. Mater.* **2004**, *16*, 4812−4818.
(27) Schubert, M.; Dolfen, D.; Frisch, J.; Roland, S.; Steyrleuthner, R.; Stiller, B.; Chen, Z.; Scherf, U.; Koch, N.; Facchetti, A.; Neher, D. Influence of aggregation on the performance of all-polymer solar cells containing low-bandgap naphthalenediimide copolymers. *Adv. Energy Mater.* **2012**, *2*, 369−380.
(28) Zhou, E.; Cong, J.; Wei, Q.; Tajima, K.; Yang, C.; Hashimoto, K. All-polymer solar cells from perylene diimide based copolymers: material design and phase separation control. *Angew. Chem., Int. Ed.* **2011**, *50*, 2799−2803.
(29) Mori, D.; Benten, H.; Kosaka, J.; Ohkita, H.; Ito, S.; Miyake, K. Polymer/polymer blend solar cells improved by using high-molecular-weight fluorene-based copolymer as electron acceptor. *ACS Appl. Mater. Interfaces* **2011**, *3*, 2924−2927.
(30) Nam, S.; Shin, M.; Kim, H.; Ha, C. S.; Ree, M.; Kim, Y. Improved performance of polymer: polymer solar cells by doping electron-accepting polymers with an organosulfonic acid. *Adv. Funct. Mater.* **2011**, *21*, 4527−4534.
(31) Nam, S.; Shin, M.; Park, S.; Lee, S.; Kim, H.; Kim, Y. All-polymer solar cells with bulk heterojunction nanolayers of chemically doped electron-donating and electron-accepting polymers. *Phys. Chem. Chem. Phys.* **2012**, *14*, 15046−15053.
(32) Ishii, H.; Sugiyama, K.; Ito, E.; Seki, K. Energy level alignment and interfacial electronic structures at organic/metal and organic/organic interfaces. *Adv. Mater.* **1999**, *11*, 605−625.
(33) Jönsson, S. K. M.; Salaneck, W. R.; Fahlman, M. Photoemission of Alq_3 and C_{60} films on Al and LiF/Al substrates. *J. Appl. Phys.* **2005**, *98*, 014901.
(34) Greczynski, G.; Fahlman, M.; Salaneck, W. R. An experimental study of poly(9,9-dioctyl-fluorene) and its interfaces with Li, Al, and LiF. *J. Chem. Phys.* **2000**, *113*, 2407−2412.
(35) Maurano, A.; Hamilton, R.; Shuttle, C. G.; Ballantyne, A. M.; Nelson, J.; O'Regan, B.; Zhang, W.; McCulloch, I.; Azimi, H.; Morana, M.; Brabec, C. J.; Durrant, J. R. Recombination dynamics as a key determinant of open circuit voltage in organic bulk heterojunction solar cells: a comparison of four different donor polymers. *Adv. Mater.* **2010**, *22*, 4987−4992.
(36) Koster, L. J. A.; Mihailetchi, V. D.; Ramaker, R.; Blom, P. W. M. Light intensity dependence of open-circuit voltage of polymer:-fullerene solar cells. *Appl. Phys. Lett.* **2005**, *86*, 123509.
(37) Chaney, R. C.; Lafon, E. E.; Lin, C. C. Energy band structure of lithium fluoride crystals by the method of tight binding. *Phys. Rev. B* **1971**, *4*, 2734−2741.
(38) Kim, Y. Power-law-type electron injection through lithium fluoride nanolayers in phosphorescence organic light-emitting devices. *Nanotechnology* **2008**, *19*, 355207.
(39) Shin, M.; Kim, H.; Kim, Y. Effect of film and device annealing in polymer:polymer solar cells with a LiF nanolayer. *Mater. Sci. Eng., B* **2011**, *176*, 382−386.
(40) Shirley, E. L.; Terminello, L. J.; Klepeis, J. E.; Himpsel, F. J. Detailed theoretical photoelectron angular distributions for LiF(100). *Phys. Rev. B* **1996**, *53*, 10296−10309.
(41) Bader, R. F. W.; Henneker, W. H. The ionic bond. *J. Am. Chem. Soc.* **1965**, *87*, 3063−3068.